



1 **Distribution and characteristics of supraglacial channels on**
2 **mountain glaciers in Valais, Switzerland**

3 Holly Wytiahlowsky¹, Chris R. Stokes¹, Rebecca A. Hodge¹, Caroline C. Clason¹, Stewart
4 S.R. Jamieson¹

5 ¹Department of Geography, Durham University, Durham, DH1 3LE, United Kingdom

6 *Correspondence to:* Holly Wytiahlowsky (holly.e.wytiahlowsky@durham.ac.uk)

7

8 **Abstract.** Supraglacial channels form a key component of glacier hydrology, transporting surface meltwater to
9 englacial and proglacial positions, which impacts ice flow dynamics, surface mass balance and the hydrochemistry
10 of glacial runoff. The presence of supraglacial channels is well-documented on ice sheets using satellite imagery,
11 but little is known about their distribution and characteristics on smaller mountain glaciers because most channels
12 fall below the resolution of freely-available satellite imagery. Here we use high-resolution (0.15 m) orthophotos
13 to delineate <2000 supraglacial channels (> 0.5 m wide) across a sample of 285 glaciers, 85 of which contain
14 channels, in Valais Canton, Switzerland, and investigate their distribution and characteristics. We find that glacier
15 hypsometry, size and slope are good predictors of drainage density, with glaciers characterised by lower relief
16 slopes (with fewer crevasses) and larger ablation areas (high meltwater supply) exhibiting higher drainage
17 densities. Drainage density is higher when glaciers terminate at mid-range elevations (2600 – 3100 m.a.s.l), likely
18 due to less surface lowering than at lower elevations, which allows channels to persist. On average, 80 % of high
19 order channels run-off supraglacially, with 20 % terminating englacially. However, there is marked inter-glacier
20 variability in where channels terminate, with 40 % of glaciers containing no englacially-terminating channels,
21 versus 3.5 % where all channels are terminate englacially. Most channels are slightly sinuous, with higher
22 sinuosities associated with large, high-order channels that are heavily incised and more likely to reactivate
23 annually. In comparison to ice sheets, the majority of channels reach the terminus supraglacially and little
24 meltwater is stored in lakes.

25

26

27

28

29

30

31



32 1 Introduction

33 Glaciers and ice caps are rapidly losing mass (Wouters et al., 2019; Hugonnet et al., 2021; Tepes et al., 2021) and
34 are anticipated to contribute to sea level rise throughout the 21st century and beyond (Bamber et al., 2019;
35 Edwards et al., 2021; Rounce et al., 2023). Glaciers in the lower latitudes (e.g., the European Alps, Caucasus,
36 New Zealand, the USA) are particularly vulnerable to atmospheric warming and may experience complete
37 deglaciation by 2100 under a strong warming scenario (e.g., RCP8.5) (Zekollari et al., 2019; Rounce et al., 2023).
38 In populated mountain regions, these changes will have profound impacts, as glaciers and snowpacks act as vital
39 water towers, supplying 1.9 billion people worldwide who live in or downstream of glacial catchments with crucial
40 freshwater (Carey et al., 2017; Zemp et al., 2019; Immerzeel et al., 2020; Sommer et al., 2020; Hugonnet et al.,
41 2021; Clason et al., 2023). Glacier meltwater responsible for feeding proglacial rivers is commonly transported to
42 the proglacial margin by supraglacial channels, with these channels forming an important component of the glacial
43 hydrological system. The presence and distribution of supraglacial channels holds implications for a range of
44 glacio-hydrological processes as they affect how efficiently meltwater is routed over, through and under glaciers,
45 along with potential to impact on suspended sediment concentrations and hydrochemistry of proglacial rivers.
46 Higher suspended sediment concentrations, for example, pose harm to downstream ecosystems and proglacial
47 reservoirs, with concentrations generally higher if meltwater is routed to the bed (Swift et al., 2002), rather than
48 transported supraglacially. Supraglacial channels also affect glacier surface mass balance because channels can
49 efficiently transport mass from the glacier as runoff. In contrast, in the absence of channels, surface melt may
50 percolate into snow or firn and refreeze. Despite the importance of meltwater routing, the controls and patterns of
51 meltwater transport on mountain glaciers remain relatively understudied. Notably, it is not fully understood why
52 the channelised flow of meltwater occurs on some glaciers but not others, nor what effect this has on glacier
53 systems (Pitcher & Smith, 2019).

54 The term ‘supraglacial stream’ was first coined in the 1970s and 1980s from observations of channels in
55 Scandinavia and the European Alps (e.g., Knighton, 1972, 1981, 1985; Ferguson, 1973; Hambrey, 1977; Seaberg,
56 1988), with their morphology often compared to terrestrial streams. However, these early studies only provided
57 small-scale, local observations of channels on individual glaciers. By comparison, a recent revival in supraglacial
58 channel research has primarily focused on large-scale remote-sensing observations of the Greenland Ice Sheet
59 (GrIS) (e.g., Smith et al., 2015; Gleason et al., 2021; Karlstrom & Yang, 2016; Yang et al., 2015, 2016, 2018,
60 2019, 2020, 2021, 2022), and to a lesser extent, Antarctica (e.g., Kingslake et al., 2017, Bell et al., 2017; Chen et
61 al., in press). Recent remote sensing techniques for channel detection on the GrIS (e.g., Yang and Smith, 2013;
62 King et al., 2016) have not been applied to mountain environments because the majority of channels are likely to
63 be below the resolution of the highest resolution satellite platforms (e.g., Sentinel-2 (~10 m), WorldView 3 (~3.7
64 m)). As a result, it is not known whether the principles that govern channel formation on larger ice sheet
65 environments also apply to mountain glaciers. The latter are characterised by typically steeper and more complex
66 topography and tend to have a larger coverage of debris cover in comparison to ice sheet surfaces.

67 Much remains unknown about channel distribution in mountainous environments, but previous research has
68 helped to establish some fundamentals about supraglacial channels (e.g., Knighton, 1972, 1981; Ferguson, 1973;
69 Yang et al., 2016). Specifically, the formation of meltwater channels is thought to occur when channel incision
70 via thermal erosion exceeds the rate of surface lowering (Marston, 1983). Channel formation is also influenced



71 by the rate of meltwater production and surface topography, with channels tending to form parallel to the steepest
72 ice flow direction (Irvine-Fynn et al., 2011; Mantelli et al., 2015). Surface topography may re-enforce itself, as
73 once an incised channel forms, the higher incision rates may result in an increasingly topographically constrained
74 channel that reactivates annually. On a smaller scale, high concentrations of channels have been suggested to be
75 correlated with high surface roughness (Irvine-Fynn, 2011), while the present of micro to macro scale surface
76 structures also influence meltwater routing (e.g., Rippin et al., 2015). Where channels occur, they are often
77 reactivated annually depending on their incised depth, which is strongly controlled by discharge rates and slope
78 (St Germain & Moorman, 2019). The most deeply incised channels are suggested to be a product of high discharge
79 or increased slope, and most commonly exhibit asymmetric cross-profiles due to the dominant direction of solar
80 radiation (St Germain & Moorman, 2019). Additionally, discharge rates are a strong control on channel
81 morphology, in particular sinuosity, with channels observed to increase in sinuosity throughout the melt season
82 (e.g., Dozier, 1976; Hambrey, 1977; St Germain & Moorman, 2019). Similar to terrestrial river networks,
83 supraglacial channels generally follow Horton's laws, meaning that higher-order channels (i.e., where the highest-
84 order is the main channel) are longer, have lower slopes, and are comprised of a lower number of channel segments
85 (Horton, 1945; Yang et al., 2016). However, much of what we know about supraglacial channels was established
86 from cold to polythermal systems or from observations of a small number of individual glaciers (e.g., Knighton,
87 1972, 1981, 1985; Gleason et al., 2016; St Germain & Moorman, 2019).

88 In this paper we investigate a range of potential controls on channel distribution and properties for a large sample
89 of glaciers ($n = 285$) in a region characterised by high melt rates. We use high-resolution (~ 0.15 m) orthophoto
90 imagery from 2020 to produce the first comprehensive inventory of almost 2,000 supraglacial channels in a
91 mountain glacier environment, with a focus on Valais Canton, Switzerland. Our aim is to characterise the
92 morphometry of supraglacial channels on mountain glaciers, providing insight into where and why they form.
93 Using GIS software, we extract channel metrics (length, sinuosity, slope, elevation, terminus type, proximity to
94 debris) and glacier characteristics (aspect, size, drainage density, elevation, crevassed extent) which are
95 supplemented by qualitative observations. Using our data, we explore the relationship between glacier and channel
96 characteristics using statistical measures and infer whether glacier surface characteristics can explain the presence
97 or absence of channels.

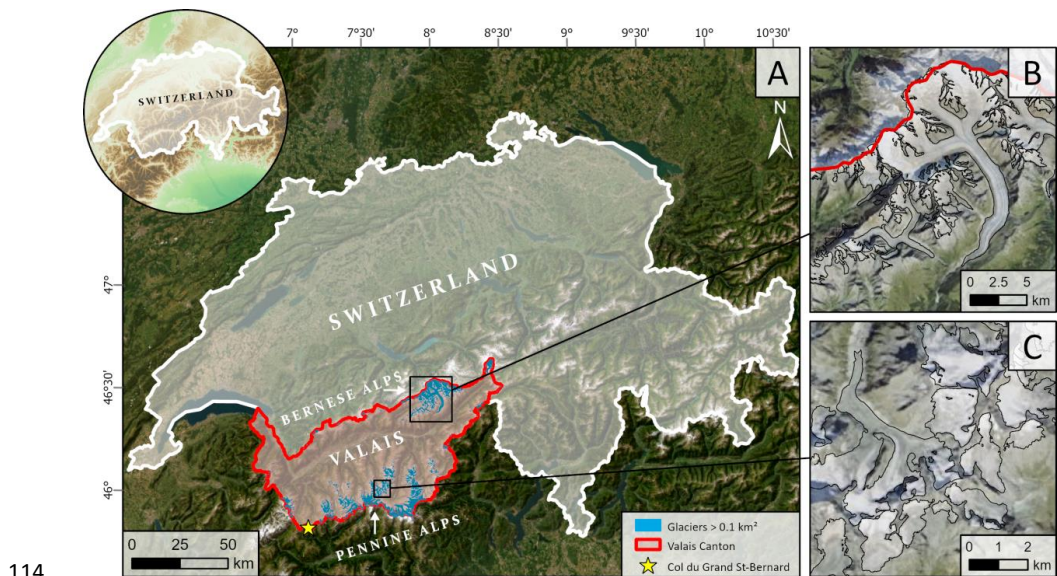
98

99 2 Study location

100 When compared to many glacierised regions, Switzerland has the largest repository of high spatial and temporal
101 resolution national LiDAR and orthophoto surveys, providing excellent coverage for the mapping of supraglacial
102 channels. We focus on Valais Canton in southern Switzerland which contains 303 glaciers over 0.1 km², covering
103 a total area of 545 km² in 2015 (Fig. 1; Linsbauer et al., 2021). It is the most glacierised Swiss Canton and in 2015
104 glaciers in Valais had a mean area of 1.8 km², a median of 0.43 km² and a maximum area of 77.3 km² (Aletsch
105 Glacier) (Linsbauer et al., 2021). We identified Valais Canton as a suitable study site as its glacier size distribution
106 is comparable with Switzerland as a whole, and the glaciers range from shallow to steep gradients, have differing
107 hypsometries (ice area-elevation distributions) and vary in crevasse densities. Thus, this study site captures a wide
108 range of potential influences on channel distributions and characteristics. Valais is comprised of the Bernese Alps



109 to the north and the Pennine Alps in the south, separated by the Rhône Valley (Fig. 1). Glaciers in the Bernese
 110 Alps are the largest in the canton and most exhibit a south-to-southeast aspect (mean: 163°). In contrast, the largest
 111 glaciers in the Pennine Alps have a north and west aspect (mean: 347°). Glaciers in Valais have an average
 112 maximum elevation of 3450 m.a.s.l (min: 2356, max: 4599) and an overall mean elevation of 3091 m.a.s.l (min:
 113 2267, max: 4025).



114
 115 **Figure 1: The study site area, which contains 303 glaciers >0.1 km². (A) The location of Valais Canton (red)**
 116 **shown within Switzerland, with glaciers shown in blue; (B) the larger glaciers (e.g., Aletsch Glacier, centre**
 117 **right) in the north of Valais Canton; and (C) the smaller glaciers in the south of Valais Canton, with varying**
 118 **levels of debris cover. The location of Col du Grand St-Bernard meteorological weather station is indicated**
 119 **by a yellow star. Glacier outlines used are from the Swiss Glacier Inventory (SGI2016), with glacier extent**
 120 **shown as of 2015-16. The outlines are overlaid on basemap imagery sourced from Esri (2024).**

121

122 Within Valais, the only meteorological station with a similar elevation to many glacier termini is Col du Grand
 123 St-Bernard (2472 m.a.s.l) in the Pennine Alps, which (between 1991 and 2020) recorded mean July air
 124 temperatures (2 m) of 8.4°C, mean January temperatures of -6.9°C, and mean annual temperatures of -0.1°C. At
 125 Col du Grand St-Bernard, July averages 140 mm of precipitation (1991-2020), with 12.7 days a month
 126 experiencing > 1 mm of precipitation, compared to a January average of 242 mm across an average of 12.9 days.
 127 The coldest temperatures are consistently recorded at Jungfraujoch (3571 m.a.s.l) in the Bernese Alps, which
 128 (between 1991 and 2020) recorded mean July air temperatures (2 m) of 0.4°C, mean January temperatures of -
 129 12.5°C, and mean annual temperatures of -7.3°C. However, Switzerland's climate is changing and mean air
 130 temperatures between 2013 and 2022 were 2.5°C warmer than pre-industrial temperatures (MeteoSwiss, 2024),
 131 which has greatly impacted the mass balance of Swiss glaciers in recent decades (Fischer et al., 2015; Davaze et
 132 al., 2020). The most recent Swiss glacier inventory (2016) records a historical glacier surface area change rate of



133 -0.6 \% a^{-1} (1973 – 2016, -350 km^2) and reveals a statistically significant acceleration of glacier area loss in the
134 Alps, with annual losses between 2010 to 2016 (-0.8 \%) having increased since 1973 to 2010 (-0.6 \%) (Linsbauer
135 et al., 2021). Volumetric losses in the Swiss Alps between 1980 and 2010 were $22.51 \pm 1.76 \text{ km}^3$, which were
136 largely concentrated between 2700 and 2800 m.a.s.l, with no elevation band experiencing positive elevation
137 changes (Fischer et al., 2015).

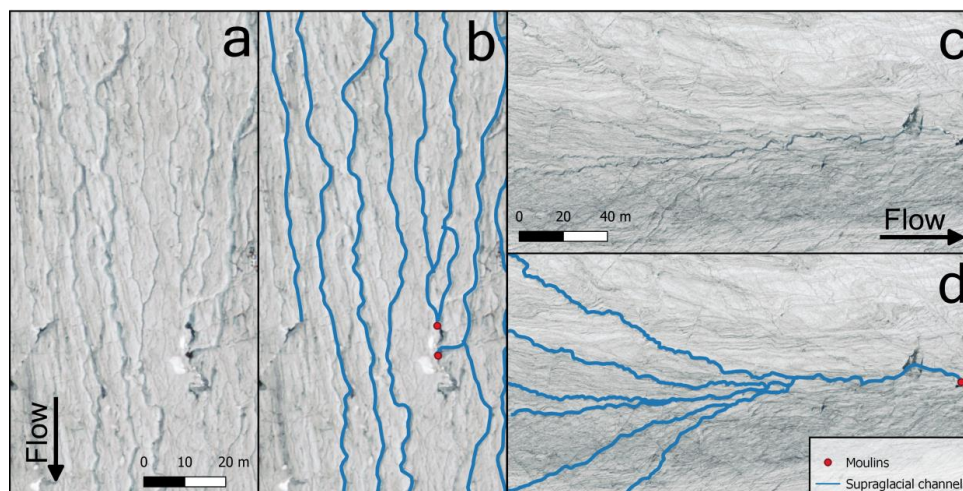
138

139 **3 Methods**

140 **3.1 Imagery acquisition and channel delineation**

141 The application of recently deployed automated methods of channel detection in ice sheet settings (e.g., Yang et
142 al., 2019) were tested at our study site and found to be insufficient for detecting the generally much smaller
143 channels. We initially applied a modified NDWI_{ice} method developed by Yang and Smith (2013) to delineate water
144 bodies from WorldView-2 imagery (1.84 m) on the Greenland Ice Sheet. However, our NDWI_{ice} output
145 predominantly detected water-filled crevasses, and only detected larger channels, missing many channels that
146 were visible, but contained very small amounts of water or incised channels where the water surface was not
147 visible. As a result, we undertook manual mapping, which in some instances has been found to be seven-fold more
148 accurate in ascertaining channel density compared to multispectral methods (King et al., 2016). We obtained high-
149 resolution cloud-free orthophoto imagery (0.15 m resolution) from SwissTopo (swisstopo.admin.ch), with
150 acquisition dates during mid-July 2020. Imagery was not available for later in the melt season; hence 6% of all
151 glacier termini were still snow-covered and were omitted from further analyses as the presence or absence of
152 channels could not be confirmed.

153 We first removed all glaciers in Valais Canton smaller than 0.1 km^2 from our study glaciers (582 reduced to 303
154 glaciers). This is because they are likely too small to produce large enough channels to be detected by our imagery,
155 and because many small glaciers in the Swiss Glacier Inventory (SGI2016) are unlikely to meet the criteria to be
156 identifiable as glaciers (Leigh et al., 2019). Once glaciers with snow-covered termini were also omitted, a total of
157 285 glaciers remain in our study site. Each glacier was then systematically surveyed for supraglacial channels in
158 *QGIS* (e.g., Fig. 2). Only channels confidently visible at a 1:1,000 scale were delineated for the purpose of
159 consistency, meaning the minimum channel width we delineated is $\sim 0.5 \text{ m}$ wide. We solely focus on these larger
160 ($>0.5 \text{ m}$) channels because of difficulties in delineating small channels objectively, which include problems with
161 differentiating complex rill networks from structural features (e.g., fractures) and the need for more subjective
162 judgments where channel width may periodically decrease beyond the pixel width. Individual channels were
163 mapped from their downstream end until they were no longer clearly visible or when channels could not be
164 confidently and objectively mapped. When channels have tributaries above the mapping resolution, the main
165 channels were mapped as one segment, continuing up the largest channel at each confluence. Each tributary
166 channel was then subsequently mapped as a new individual segment. Once mapped, each entire channel segment
167 was assigned codes based on its attributes, i.e., where it terminated (e.g., terminus, moulin, crevasse, lake,
168 periphery, adjoins another channel, disappears beyond the resolution), and whether it was on bare ice or a debris-
169 covered part of the glacier.



170

171 **Figure 2: Examples of the mapped output and corresponding orthophoto. Channels are shown in blue, and**
172 **moulins are represented as red circles when a mapped channel is moulin terminating. (a - b) Supraglacial**
173 **channels on the Rhone Glacier and (c-d) Allalin Glacier. Imagery source: Federal Office of Topography**
174 **swisstopo.**

175

176 3.2 Metrics

177 A total of 1890 channel segments (polylines) were mapped across 85 glaciers found to contain channels. We then
178 used the high-resolution (0.5 m) SwissALTI3D DEM (2019) from swisstopo.admin.ch (1 sigma accuracy of ± 0.3
179 m for each dimension) to extract morphometric characteristics from each channel segment. The DEM is coarser
180 than the orthophotos used for channel delineation and there is a one-year offset between their acquisition dates.
181 However, as the DEM is used to calculate larger scale metrics such as elevation and slope, the small offset is
182 unlikely to affect overall results. Channel metrics extracted were segment length, straight line distance, elevation
183 (minimum, maximum), elevation difference and channel slope. The start and end point of each segment were then
184 used to derive the sinuosity of each segment (channel length/straight line distance) and drainage density for each
185 glacier (total length of channels/glacier area). We use the glacier snow-free area at the time of mapping to calculate
186 drainage density, which results in a higher value than if the entire glacier area was used.

187 Glacier characteristics were obtained from the Swiss Glacier Inventory (SGI2016), which provided information
188 on glacier area, aspect, and elevation (minimum, maximum and mean) in 2015 (Linsbauer et al., 2021). This
189 record is used as it is the most up-to-date record of Swiss glacier area, but glaciers have since undergone substantial
190 recession. The values for glacier slope from the SGI2016 cannot be used as they encompass the whole glacier,
191 whereas for our analysis we wanted to measure the slope of the snow-free portion of the ablation area at the time
192 of channel mapping. To calculate slope values, each glacier polygon was clipped to its snow-free area, and then
193 zonal statistics in *QGIS* were used to extract the mean, minimum and maximum slope value from the
194 SwissALTI3D DEM for each polygon. The snow-free slope value is the only glacial slope value used in data



195 analyses. Upon completion of mapping, we assigned codes to each glacier based on the extent of debris cover and
196 crevassed area due to their potential controls on channel formation. Glacier debris cover is visually estimated and
197 allocated to one of five classes (none, <10 %, 10-25 %, 25-50 % and >50 %) and crevassed area is assigned to
198 one of three classes little to none (less than 10 % of the ablation area), moderate (10-50 % covered), and heavily
199 crevassed (covers >50 % of the ablation area).

200

201 3.3 Statistical tests

202 To determine whether there is a relationship between channel morphometry and glacier characteristics, we
203 produced a correlation matrix using Spearman's rank correlation (ρ) (e.g., St Germain & Moorman, 2019). Each
204 metric used in this analysis comprises 1890 values, each representing an individual channel segment. The analysis
205 used the following channel variables: segment length, channel slope, sinuosity, minimum elevation, maximum
206 elevation and elevation range, and the following glacier variables: drainage density, glacier area, mean slope of
207 the snow-free area, aspect, glacier minimum elevation, glacier mean elevation and glacier maximum elevation.
208 For each of the glacier variables, all channel segments on the same glacier are allocated the same value. A singular
209 ANOVA test was conducted to determine the significance of the relationship between debris cover and sinuosity
210 as an ANOVA test is best suited to determining if there is a significant difference between different classes of
211 debris cover. We also conducted a Principal Component Analysis (PCA) to determine the relationship between
212 variables and to identify drivers of variance amongst the dataset, with data normalised to aid in identifying patterns
213 within the data.

214

215 4 Results

216 4.1 Glacier observations

217 The study area contained 285 glaciers with an area over 0.1 km² and a snow-free terminus in 2020 (Linsbauer et
218 al., 2021). Of these, 85 glaciers were found to have supraglacial channels above the mapping resolution (~0.5 m).
219 Glaciers with channels (n = 85) have a mean area of 5 km² and glaciers without channels (n = 200) have a mean
220 area of 0.6 km². However, glacier area frequency distributions peak in the 0.1 to 1 km² category for both glaciers
221 with and without channels (Fig. 3a). All glaciers larger than 5.6 km² were found to contain channels (Table 1, Fig.
222 3a). Where channels are present, glaciers have an overall mean slope of 21° and a maximum mean slope of 43°,
223 with glacier slope being positively skewed towards lower slope values (Table 1, Fig. 3b). By comparison, where
224 channels are absent, glaciers are characterised by steeper overall slopes (mean: 28°, max: 45°) (Fig. 3b).

225 Glaciers without channels are more likely to terminate at higher elevations (mean minimum elevation: 2936 m)
226 compared to glaciers with channels (mean minimum elevation: 2797 m), which are often characterised by longer
227 valley glacier tongues. Where glaciers support channels, they are more likely to have a higher maximum elevation
228 (mean max elevation: 3637 m) than glaciers without channels (mean max elevation: 3555 m). Where channels are
229 present, there is a mean drainage density of 2.4 km/km² and a maximum of 15.2 km/km². The latter was found on
230 the Upper Theodul Glacier, which is situated on a low slope plateau and has the lowest glacier slope angle in the

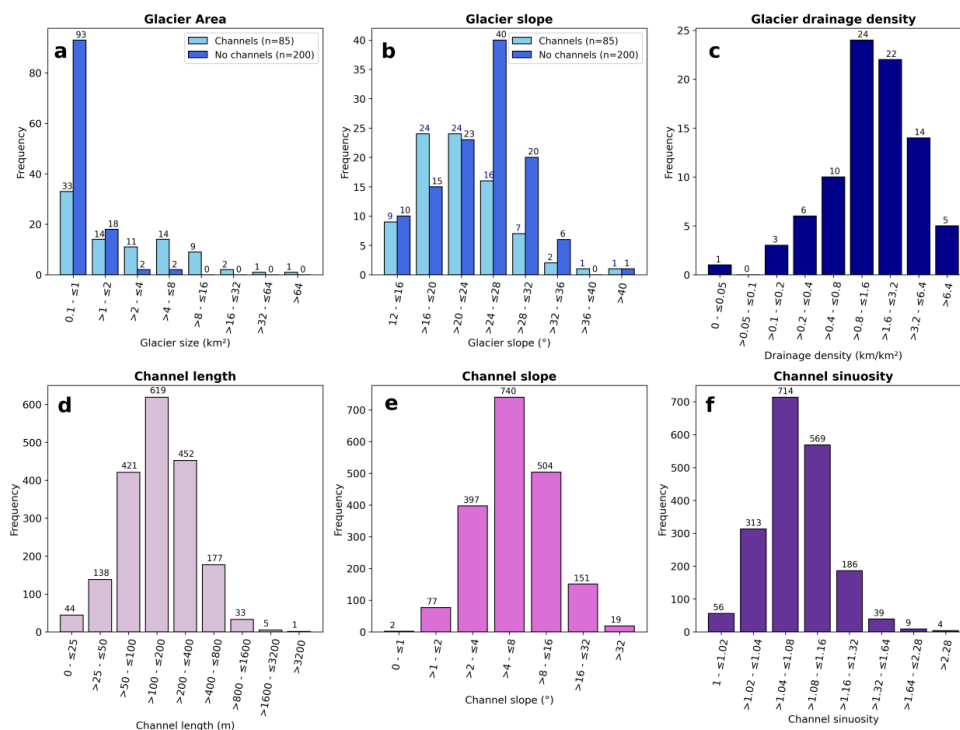


231 dataset (13°) (Fig. 3c, Fig. 4a). To summarise, glaciers containing channels are larger, have lower mean slopes,
232 and have a larger portion of their area at lower elevations compared to glaciers without channels.

233 **Table 1: A quantitative summary of glacier and channel characteristics.**

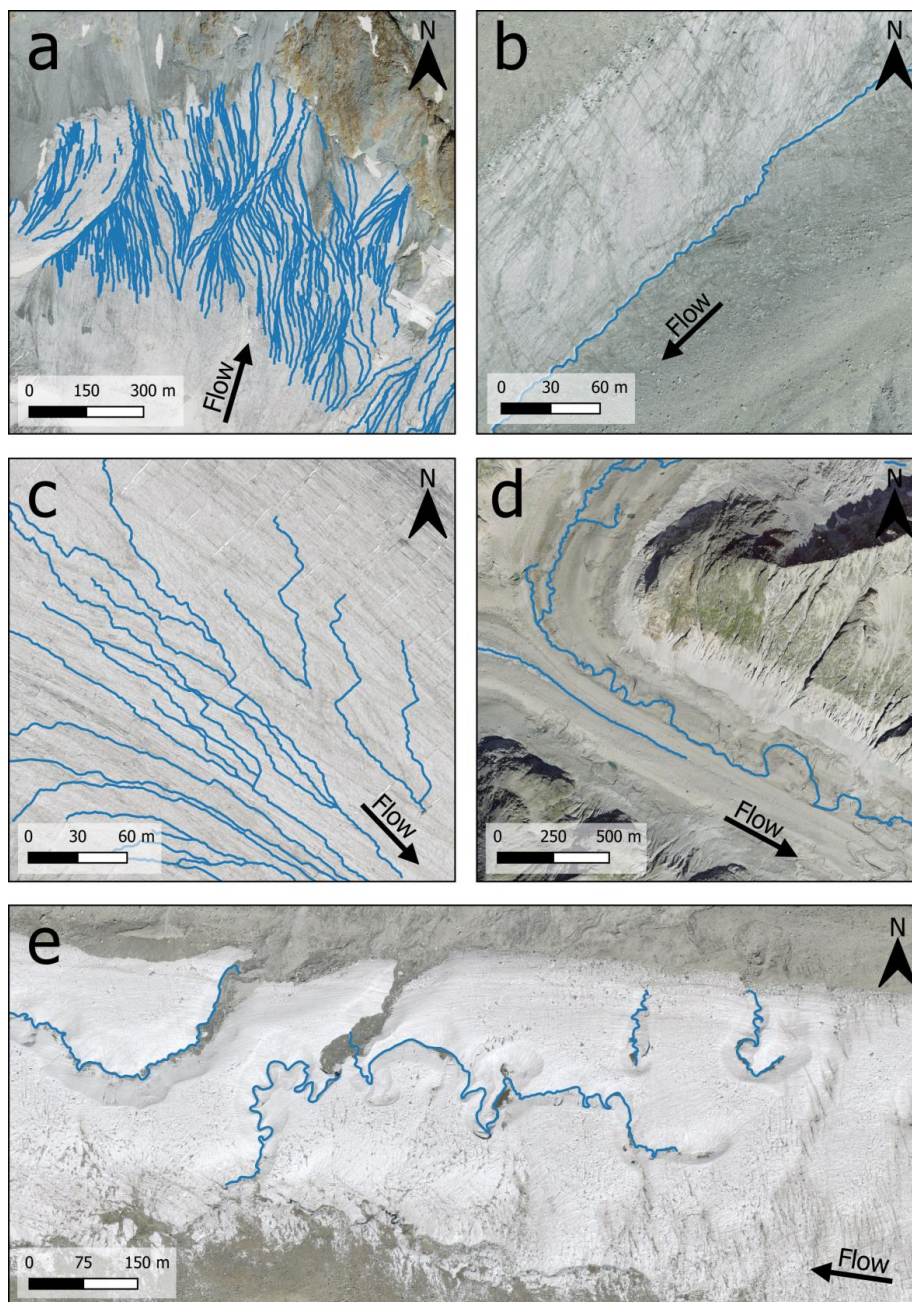
	Channel Length (m)	Channel Slope (°)	Sinuosity	Drainage Density (km/km ²)	Mean Glacier Slope (°)	Glacier Area (km ²)
Count	1890	1890	1890	85	85	85
Minimum	5.2	0.8	1.0	0	10.4	0.1
Median	152.2	6.3	1.1	1.5	20.6	1.5
Mean	211.7	8.0	1.1	2.4	21.0	5.0
Maximum	4314.4	47.8	3.8	15.3	43.0	83.0
Range	4309.3	47.0	2.8	15.2	32.6	82.9
Standard Deviation	228.3	6.3	0.1	2.6	6.5	10.7
Standard Error	5.3	0.1	0.0	0.3	0.7	1.2
Kurtosis	65.8	7.4	153.0	9.0	1.1	35.3
Skewness	5.5	2.3	9.5	2.6	0.8	5.4

234



235

236 **Figure 3: Histograms of extracted metrics. Note that the x-axis is log a scale (except for Fig. 3b) and the**
 237 **numbers above each bar represent the number of channels/glaciers within each class. (a) Glacier area**
 238 **(km²); (b) glacier slope (°); (c) glacier drainage density (km/km²); (d) channel length (m); (e) channel slope**
 239 **(°); and (f) channel sinuosity.**



240

241 **Figure 4: Examples of supraglacial channels. (a) Channels on the Upper Theodul Glacier; (b) a channel at**
242 **the interface between bare ice and debris-covered ice on Glacier du Brenay; (c) channels on the Great**
243 **Aletsch Glacier - note the straight segments where crevasses have been exploited; (d) channels on the debris-**
244 **covered terminus of the Upper Aletsch Glacier; and (e) sinuous channels towards the terminus of Gorner**
245 **Glacier. Flow indicates the glacier flow direction. Imagery source: Federal Office of Topography swisstopo.**



246 **4.2 Channel characteristics**

247 Individual channel segments have a mean length of 212 m, with a positively skewed leptokurtic distribution (Fig.
248 3d; Table 1). Few segments exceed 1,600 m as the length of most glacier's ablation area is smaller than this value.
249 The channel segments have a mean slope of 8°, and most exhibit a slope between 4 to 16° (Fig. 3e; Table 1). The
250 maximum channel slope observed is 48°, but the overall distribution is positively skewed towards smaller slope
251 values. The sinuosity index of each channel ranges from 1 (straight line) to a maximum of 3.8, with a mean value
252 of 1.1, which is slightly sinuous, but not high enough to be defined as meandering (Table 1). Sinuosity is the most
253 positively skewed variable, with a highly leptokurtic distribution, as most channels are not very sinuous (Fig. 3f).

254 Channels terminate in a range of settings, with 47 % joining another channel, 15 % terminating in crevasses, 14
255 % terminating in moulins, 13 % disappearing below the mapping resolution, 8 % running off at the glacier
256 terminus, 2 % running off the side of the glacier, and 1 % terminating in a supraglacial lake. When only considering
257 terminal segments, 72 % of segments terminate englacially (crevasses or moulins), 25 % run-off (terminus or
258 periphery), and 3 % terminate in a supraglacial lake. However, larger glaciers with higher drainage densities
259 disproportionately impact on these values. For example, 582 out of the 1890 mapped channel segments are on the
260 Aletsch Glacier, where no channels reach the terminus, hence englacially terminating channels may be
261 overrepresented by a singular glacier. Thus, when the percentage of channels terminating in each position are
262 extracted as an average value from each glacier, 80 % of channels reach the terminus supraglacially and 20 % of
263 channels terminate englacially. Overall, 48 % of glaciers have no englacially-terminating channels, with only 3.5
264 % of glaciers that solely contain englacially terminating channels.

265 Where channels occur, qualitative observations indicate structural and topographic controls on their distribution
266 and morphology. For example, large channels often occur at the interface between debris-covered and bare ice
267 (e.g., Fig. 4b), particularly adjacent to medial moraines, where they are confined to a topographic depression,
268 commonly occurring at the confluence between two tributaries. The influence of glacier structure on channel
269 morphology is also observed where trace or shallow crevasses are exploited to produce long, straight channel
270 sections (e.g., Fig. 4c). By comparison, the most sinuous channels tend to occur at lower elevations on large
271 glaciers characterised by larger flat areas towards to their terminus (Fig. 4e).

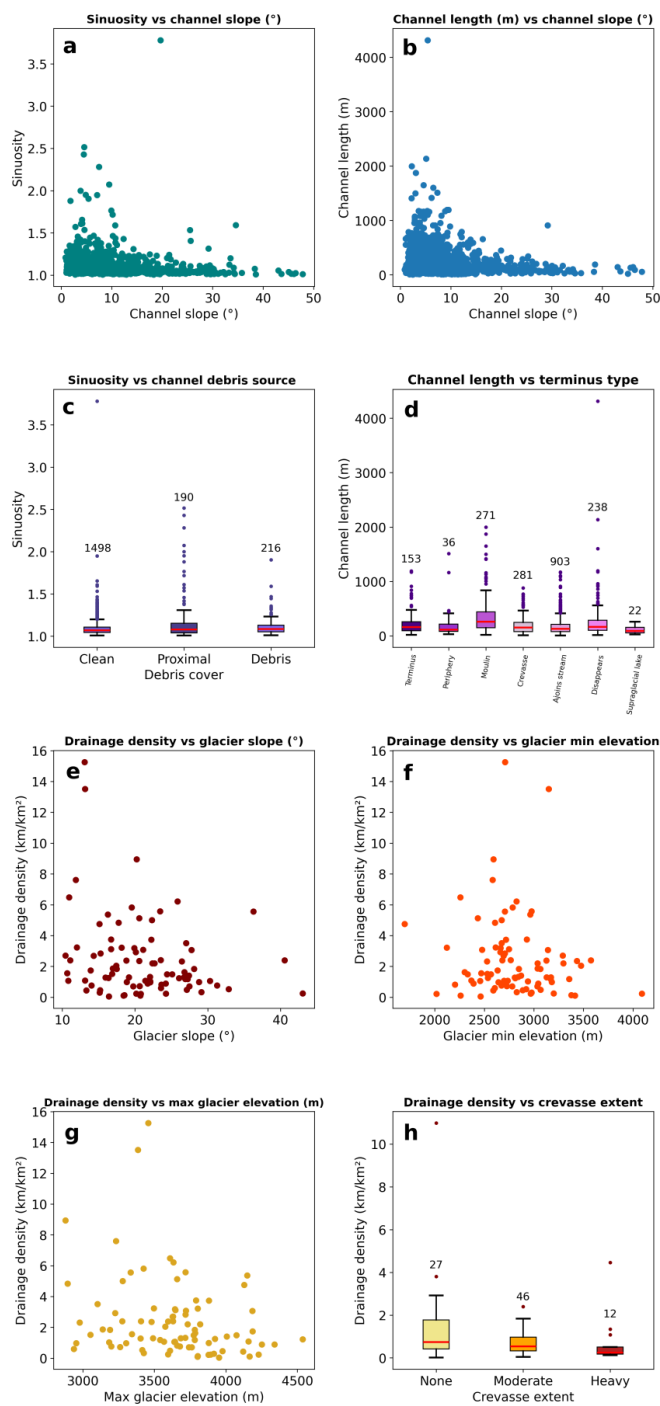
272

273 **4.3 Controls on channel morphology and distribution**

274 To investigate whether there are links between different supraglacial channel characteristics, we plotted our
275 extracted metrics against each other (Fig. 5). Previous studies informed our choice of variables tested for potential
276 relationships, with a focus on how glacier properties (slope, area and elevation) affect glacier drainage density
277 (e.g., Yang et al., 2016) and channel morphology, such as sinuosity and channel length (e.g., St Germain &
278 Moorman, 2019). We found that the most sinuous channels are most likely to occur on lower glacier slopes (0 to
279 10°), with a clear upper boundary demonstrating that channels on steeper slopes (> 20°) are unlikely to exhibit a
280 sinuosity over 1.2 (Fig. 5a). A relationship between channel segment length and slope is also apparent, with the
281 longest channel segments occurring on the lowest slope angles, which often have a lower density of crevasses
282 (Fig. 5b). This relationship is clearly defined by an upper limit, indicating slope is a clear control on both channel



283 length and sinuosity (Fig. 5a-b). We find no noticeable difference in sinuosity between channels on bare ice and
284 those on debris-covered glaciers (Fig. 5c). However, channels proximal to debris (i.e., channels which are likely
285 to have some sediment content) are more likely to be highly sinuous than channels on bare ice or continuous
286 debris cover, with differences between the classes statistically significant ($p = <0.05$) in an ANOVA test (Fig. 5c).
287 Channel segments that terminate in moulins tend to be the longest (mean: 341 m, max: 1999 m), followed by
288 channels that disappear below the mapping resolution (mean: 259 m, max: 4314 m), and then channels reaching
289 the glacier terminus (mean: 214 m, max: 1193 m) (Fig. 5d). The very few (1 %) channels that terminate in
290 supraglacial lakes tend to be short (mean: 109 m, max: 260 m), along with channels that adjoin a higher-order
291 channels (mean: 169 m, max: 1174 m) (Fig. 5d).



292

293 **Figure 5: Relationships between channel characteristics (a-d) and glacier metrics (e-h). Plots a-d contains**
 294 **data from 1890 channels, and plots e-h contain data for the 85 glaciers with channels. (a) Sinuosity vs**



295 **channel slope (°); (b) channel length vs channel slope (°); (c) sinuosity vs channel debris source; (d) channel**
296 **length (m) vs terminus type; (e) drainage density (km/km²) vs glacier slope (°); (f) drainage density**
297 **(km/km²) vs minimum glacier elevation; (g) drainage density (km/km²) vs maximum glacier elevation (m);**
298 **and (h) drainage density (km/km²) vs crevasse extent.**

299

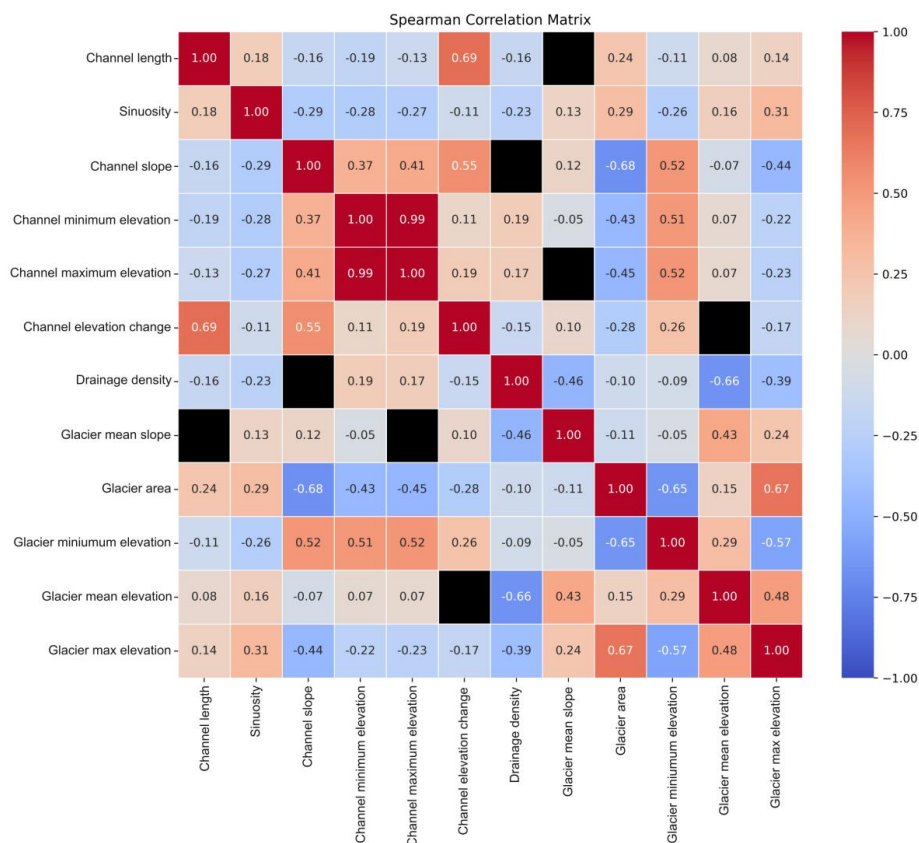
300 The influence of glacier characteristics on channel characteristics is less evident, perhaps due to the lower number
301 of data points. However, a relationship between drainage density and glacier slope exists, with the highest drainage
302 densities occurring on the lowest surface slopes (Fig 5e). Glaciers with high drainage densities tend to have a
303 minimum elevation range between 2600 and 3100 m.a.s.l (Fig. 5f), whereas a relationship between drainage
304 density and maximum elevation is less evident (Fig. 5g). However, the very highest drainage densities tend to
305 occur where glaciers have a lower maximum elevation (Fig. 5g). Additionally, the crevassed extent of a glacier
306 affects drainage density, as increased channel inception prevents the formation of longer channels (Fig. 5h).

307

308 **4.4 Spearman's rank and principal component analysis**

309 We examined the controls on channel morphology and drainage density by calculating a correlation matrix. We
310 use Spearman's rank correlation (ρ) and significance values (p), given that many of our relationships do not appear
311 linear. Additionally, given the large sample size within our dataset and that most p-values are < 0.05 , relationships,
312 including weak ones, are significant.

313 The strongest control on glacier drainage density is identified to be glacier mean elevation ($\rho = -0.66$, $p = \leq 0.001$),
314 with higher drainage densities present when a larger portion of glacier mass exists at lower elevations (Fig. 6).
315 This is followed by glacier mean slope ($\rho = -0.46$, $p = \leq 0.001$), with higher drainage densities on glaciers
316 characterised by a lower mean slope. This is consistent with Fig 7e, with the highest drainage densities observed
317 at glaciers with very low slope angles (e.g., the Upper Theodul Glacier; Fig. 4d).



318

319 **Figure 6: A heatmap matrix of Spearman's rank correlation to show the relationship between glacier and**
 320 **channel characteristics. Correlation values are scaled along a colour ramp and non-significant relationships**
 321 **($p > 0.05$) are coloured black.**

322

323 By comparison, channel morphology is characterised by more complex and weaker relationships between
 324 variables. For example, high channel sinuosity can in part be explained by multiple weak correlations: sinuosity
 325 values tend to increase with a decrease in channel slope ($\rho = -0.29, p = \leq 0.001$), and the most sinuous channels
 326 occur on larger glaciers ($\rho = 0.29, p = \leq 0.001$) with lower minimum elevations ($\rho = -0.26, p = \leq 0.001$) (Fig. 6).
 327 Lower relief surfaces are often found when valley glaciers extend down-valley to flatter terrain, supported by
 328 observations of highly sinuous channels on low slope glacier tongues (e.g., Gorner Glacier) (Fig. 4e). The channel
 329 slope is primarily controlled by glacier characteristics, with higher slope channels mostly existing on smaller
 330 glaciers ($\rho = -0.68, p = \leq 0.05$), which terminate at higher elevations ($\rho = 0.52, p = \leq 0.05$), meaning the steepest
 331 channels are likely to be found at high elevation cirques and hanging glaciers.

332 To assess the relationship between variables and determine the drivers of variance, we conducted a Principal
 333 Component Analysis (PCA) (see Appendix 1). The PCA loadings show that glacier area has a large negative



334 loading on principle component 1, closely followed by strong positive loadings from minimum glacier elevation
335 and channel elevation (maximum and minimum). By comparison, principal component 2 shows a strong positive
336 loading from drainage density, and large negative loadings from mean glacier slope and glacier mean elevation.
337 The first two components explain 50 % of the variance within the dataset, with an additional 13 %, 12 % and 9 %
338 explained by principal components 3, 4 and 5, respectively, which together explain 84 % of the variability. Given
339 the complexity of the dataset, our cluster analysis reveals no clear clustering of data, but the PCA loadings show
340 an expected relationship between elevation variables and slope variables, with variables such as drainage density
341 not closely related to a singular other variable. Overall, our PCA analysis reveals no singular driver of variance,
342 instead, it is apparent that there is a complex, yet interlinked relationship between all variables that explain the
343 distribution and appearance of supraglacial channels.

344

345 **5 Discussion**

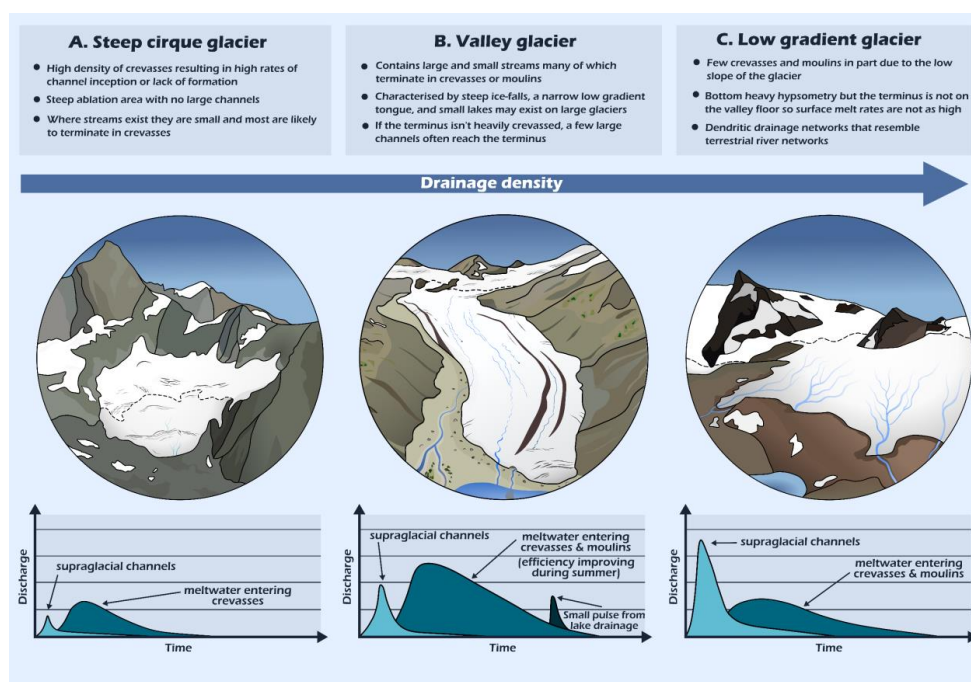
346 **5.1 Controls on the spatial distribution of channels**

347 Out of 285 glaciers examined within our study area, we find that 85 contain channels (>0.5 m) using high-
348 resolution imagery (0.15 m) from mid-July 2020. The presence of channels above our mapping threshold (>0.5 m
349 wide) is primarily controlled by a combination of sufficient meltwater supply and distance for meltwater to
350 coalesce and incise. Hence, in mountain glacier environments, larger channels are infrequently detected on cirque
351 glaciers due to their smaller ablation area, steeper and often crevassed slopes, and limited distance for meltwater
352 to coalesce. By comparison, all glaciers in Valais larger than 5.6 km² supported channels, but there is a large
353 variation in drainage density. This variation is in part attributed to glacier slope, which together with ice flow
354 velocity, governs the crevassed area of a glacier, restricting the area in which channels can form. Crevasses can
355 either intercept meltwater, transporting water englacially and inhibiting the formation of longer channels or instead
356 can route water along a trace crevasse as part of a channel depending on crevasse depth. Additionally, channel
357 formation is also governed by glacier hypsometry, with glaciers characterised by bottom-heavy hypsometries more
358 likely to produce higher drainage densities due to a larger ablation surface area. Figure 7 shows a schematic of
359 how the different elevation and hypsometry of glaciers is likely to influence the distribution and density of
360 supraglacial channels in the study area.

361 Whilst valley glaciers might extend down to low elevations, they often do not have the highest drainage densities
362 because channel formation may be restricted by small valley widths and higher rates of surface lowering (Fig. 7).
363 For example, the highest drainage densities occur on the Upper Theodul Glacier, which has a low relief slope, is
364 situated on a plateau above the valley floor, and has a wide ablation area (Fig. 4a). It is possible that because the
365 Upper Theodul Glacier is situated on a higher elevation plateau, air temperatures at the terminus are likely to be
366 cooler than at the terminus of neighbouring glaciers which extend further down valley. As a result, the rate of
367 surface lowering is likely lower, meaning that lower rates of incision are needed for channel formation to keep
368 apace with surface lowering, resulting in a higher drainage density (Rippin et al., 2015; Pitcher & Smith, 2019).
369 However, summer temperatures in the Alps are increasing (Sommer et al., 2020), which will result in higher rates
370 of surface lowering, meaning that glaciers extending to lower elevations will require increased channel incision
371 to counteract the higher rates of surface lowering in order for channel formation.



372



373

374 **Figure 7: A schematic depicting the range of glacier types (A-C) and their respective characteristics,**
 375 **increasing in drainage density from left to right. Each glacier type corresponds to a predicted hydrograph**
 376 **(bottom) depicting changes in proglacial channel discharge as a response to surface melt. Light blue shading**
 377 **shows the conceptual hydrograph if all of the meltwater were to be transported via supraglacial channels,**
 378 **whereas those shown in mid-blue show the hydrograph where the bulk of meltwater is transported**
 379 **englacially/subglacially. Dark blue in panel (b) shows a lake drainage event.**

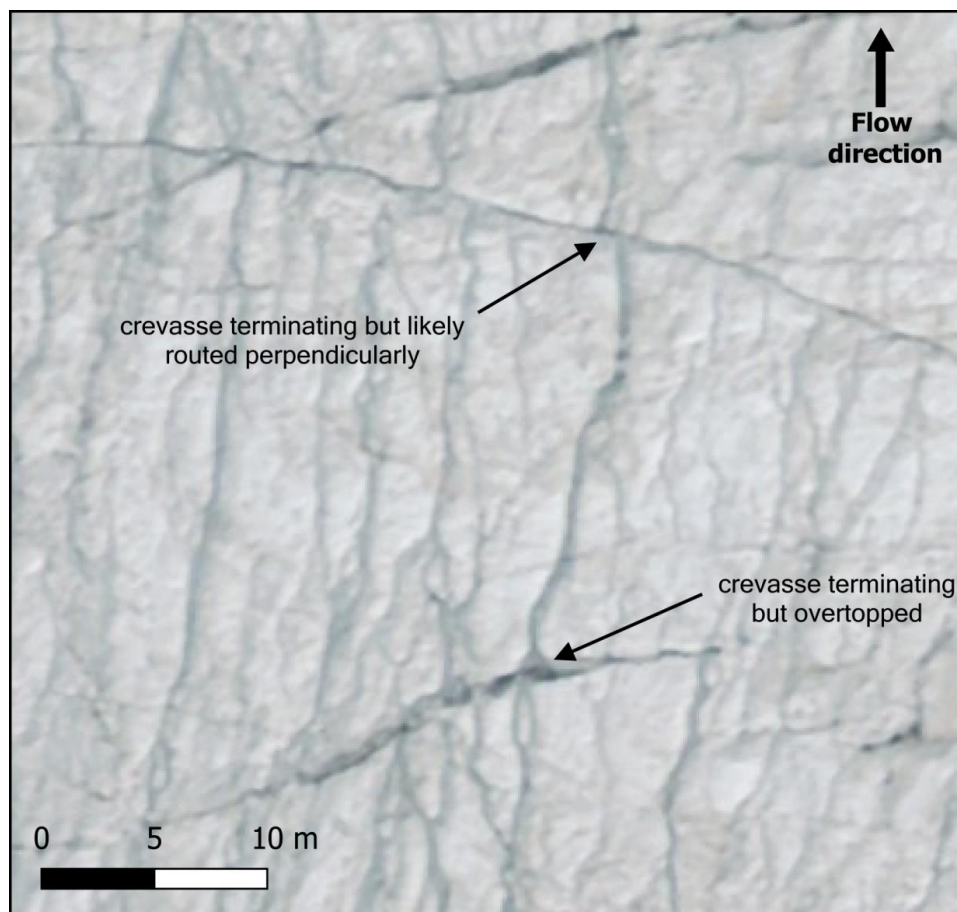
380

381 The distribution/density of channels on different types of glaciers is also likely to impact on the runoff hydrograph
 382 (Fig. 7). Small cirque glaciers (Fig. 7A) are typically characterised by steep, heavily crevassed slopes, meaning
 383 meltwater is more likely to be captured by crevasses, and there is limited distance for meltwater to coalesce and
 384 form channels. Hence, run-off at cirque glaciers in response to surface melt is likely characterised by a small
 385 earlier peak from a few supraglacial channels (light blue shading in Fig. 7A) or a slightly delayed peaks as
 386 crevasses capture meltwater and route it through the en- (and -sub) glacial system (dark blue shading in Fig. 7A).
 387 By comparison, valley glaciers are frequently characterised by larger non-crevassed zones, meaning more
 388 meltwater reaches the terminus supraglacially, but channels are often intercepted by crevassed zones or ice falls.
 389 This results in an initial peak from supraglacial channels, followed by a delay in meltwater routed en- (and sub-)
 390 glacially (Fig. 7B), with a progressively reduced lag time throughout the melt season due to increased subglacial
 391 drainage network efficiency (Nienow et al., 1998). Additionally, some larger valley glaciers contain small lakes
 392 (e.g., Gorner Glacier and Aletsch Glacier), which may experience infrequent drainage events, leading to a sudden



393 peak in proglacial river discharge. Whilst less common in Valais, glaciers characterised by large low relief ablation
394 areas often contain large supraglacial drainage networks that capture the majority of surface melt due to having
395 smaller and fewer crevasses than most valley glaciers (Fig. 7C). They will tend to have the ‘flashiest’ hydrograph
396 because the supraglacial drainage network rapidly transfers melt off the glacier surface. Where a small number of
397 crevasses or moulins intercept this drainage, it leads to a more lagged hydrograph response and with a peak well
398 below the hydrograph from supraglacial channel drainage.

399 Our dataset provides new insight into meltwater transport across a large range of glaciers, allowing simple
400 inferences to be made about connectivity and lag times. Overall, we find that 72 % of our mapped main stem
401 segments route meltwater to en- or subglacial positions and 25 % run off at the glacier margin. However, this
402 varies between glaciers and in the case of the largest glacier, the Aletsch Glacier, no mapped channels reach the
403 terminus, attributed to the location of highly crevassed zones, forcing meltwater into the glacier (53 % of channels
404 enter moulins and 36 % enter crevasses). Unlike most glaciers in the Alps, small supraglacial lakes are also present
405 on the Aletsch glacier, which capture 11 % of channels. By comparison, the Upper Theodul glacier, which exhibits
406 the highest drainage density within our dataset, contains almost no moulins (2.8 % of channel termination) and
407 27 % of channels reach the terminus or periphery, compared to 0 % at the Aletsch glacier. A large number of
408 channels terminate in crevasses on the Upper Theodul Glacier (70 %), but crevasses tend to be small (<0.3 m
409 wide) and may not route the meltwater en- or sub-glacially but rather may act as part of the channel network and
410 are mapped as individual segments as they may not be continuous. Instead, crevasses may fill with meltwater and
411 be overtopped or route meltwater perpendicular to the ice flow direction (Fig. 8). We attribute the difference in
412 drainage pathways to the low slope of the Upper Theodul Glacier, its smaller glacier area, and the lack of high-
413 density crevasse fields or ice falls, meaning meltwater is more likely to be transported via channels to the terminus
414 (e.g., Fig. 7C). This likely results in drastically different lag times within a given day between the two glaciers,
415 with the Upper Theodul likely experiencing an initial peak from run-off at the terminus, whereas at the Aletsch
416 Glacier the delay between surface melt and proglacial discharge will be larger due to longer pathways and the
417 potential for supraglacial and subglacial storage (Hock et al., 1999) (e.g., Fig. 7B). Additionally, at Aletsch Glacier
418 the high portion of moulin and crevasse terminating channels likely contributes to the seasonal speed-up in ice
419 flow velocity when meltwater reaches the bed (Leinss and Bernhard, 2021). By comparison, the supraglacial and
420 subglacial system are anticipated to be less coupled at the Upper Theodul Glacier. Hence, the characteristics of
421 these glaciers (e.g., heavily crevassed areas, presence of moulins) and the channel terminal positions may help
422 provide simple insight into surface-to-bed connectivity but would need to be verified by fieldwork. Understanding
423 these variations in meltwater routing is important because increased interaction between meltwater and the glacier
424 bed can impact subglacial erosion rates and sediment transport out of glacial systems, which in regions such as
425 the Alps can directly impact agriculture and hydropower infrastructure. For example, Delaney et al. (2020) found
426 that increased meltwater at the bed is likely to increase sediment discharge despite a reduction in ice flow velocity
427 under climatic warming and resulting glacier thinning. However, freshwater flux from supraglacial channels that
428 terminate in lateral or proglacial positions may dilute sediment loads.



429

430 **Figure 8: Examples of channels terminating in crevasses on the Upper Theodul Glacier. Channels are shown**
431 **to terminate in crevasses but often continue directly down-glacier as some meltwater overtops the crevasse.**

432 **Imagery source: Federal Office of Topography swisstopo.**

433

434 5.2 Controls on channel morphology

435 In Valais Canton, we observe a broad range of channel characteristics (e.g., Fig. 4), with sinuosity of particular
436 interest due to the similarities with alluvial fluvial systems. However, the mechanisms of meandering in ice-walled
437 channels are less likely to result from the erosion and deposition of sediment which occurs in fluvial systems
438 (Knighton, 1972). Instead, in supraglacial environments, meander evolution is thought to occur by a combination
439 of thermal erosion and downcutting, with incision rates tending to be highest on steeper slopes (Gulley et al.,
440 2009). The role of glacier slope in controlling channel sinuosity is particularly evident in Valais (Fig. 5a),
441 demonstrating a clear upper limit where highly sinuous channels are unlikely to occur on higher relief slopes (e.g.,
442 over 20°). However, this figure may also reflect the preferential area for larger channels to form (i.e., flatter, less
443 crevassed regions) rather than the direct impact slope has on sinuosity. This may explain the difference in the



444 influence of slope on sinuosity between Valais and in the high Arctic, where St Germain & Moorman (2019)
445 attribute higher channel sinuosity to higher relief slopes and increased channel discharge. As cold-based glaciers
446 tend to be less crevassed and dynamic, the viable area for channel formation (i.e., less highly crevassed zones) is
447 likely to be higher per glacier than in Valais. It is anticipated that the role of discharge remains similar in both
448 environments, as our observations find that larger channels (higher discharge) tend to be more sinuous (e.g., Fig.
449 4d-e). The sinuous channels observed by St Germain & Moorman (2019) are typically highly incised, meaning
450 they tend to persist inter-annually. However, in our study area, the rates of surface lowering are likely to be much
451 higher, meaning a larger proportion of channels might melt out/disappear if their rate of incision is less than the
452 rate of surface lowering. The exception being large highly sinuous channels, which are likely to persist longer
453 term due to their higher discharge and subsequent increased rates of incision.

454 Compared to bare-ice glaciers, supraglacial channels on debris-covered glaciers are commonly highly incised,
455 with channel pathways influenced by local-scale glacier surface topography (e.g., medial moraines). For example,
456 we observe some cases where less sinuous channels are funnelled through thin areas of exposed bare ice, until
457 reaching continuous debris-cover, where large meandering planforms begin to develop (e.g., Fig. 4d). In addition,
458 there is a general absence of small channels on debris-covered glaciers in Valais due to slow and dispersed
459 meltwater transport through the debris matrix (Fyffe et al., 2019), with predominantly incised canyon-like
460 channels present. Unlike debris-free glaciers, incised channels in debris-cover form exposed banks of bare ice
461 which are too steep to harbour debris and are distinct from the thick debris covered surface. Whilst the melt rates
462 are much lower beneath continuous debris cover (Kneib et al., 2023; Fyffe et al., 2019), once bare ice is exposed
463 by channel incision, meltwater production is increased due to exposure of non-insulated ice (Mölg et al., 2019),
464 with increased discharge likely furthering channel development.

465 Additionally, increased sediment presence within channels, which would be expected on highly debris-covered
466 glaciers, can increase the water temperature due to inhibiting heat exchange between the meltwater and the channel
467 wall (Isenko et al., 2005). The combination of higher water temperatures and debris-covered glaciers often means
468 that most of their surface melt is concentrated in a few channels (i.e., higher channel discharge) and likely results
469 in very high rates of channel incision, producing these high amplitude meanders that are not observed on bare ice
470 glaciers in Valais. However, the role of debris in supraglacial channels is poorly understood as most supraglacial
471 research has occurred on ice sheets, where areas of lower albedo are controlled by the presence of, dust, black
472 carbon, algae, and cryoconite deposits (Ryan et al., 2018; Leidman et al., 2021; Khan et al., 2023).

473 Further insight may be gained from bedrock rivers, which contain a mixture of sediment cover and exposed
474 bedrock. In bedrock rivers, sediment was found to increase channel erosion rates and increase sinuosity, but high
475 sediment supply may reduce erosion due to producing sediment cover which protects the bed from erosion (Moore,
476 1926; Shepherd, 1972; Turowski, 2018). Ultimately, future work is needed to determine the role of debris in
477 supraglacial systems, specifically in situ measurements of debris content in channels to determine how it affects
478 channel properties.

479



480 **5.3 Comparison between mountain glaciers and ice sheets**

481 Supraglacial channels are an important component of glacier hydrology in both mountain glacier and ice sheet
482 settings, yet some obvious differences exist between the two environments. The difference in scale means that in
483 an ice sheet setting, particularly at less crevassed higher elevations, there is sufficient distance for meltwater to
484 incise and channels to coalesce forming established drainage networks, which broadly follow Horton's laws i.e.,
485 mean river length increases with channel order and mean slope decreases with channel order (Yang et al., 2019).
486 In contrast, whilst interconnected dendritic networks do occur on mountain glaciers (e.g., Fig. 5a), they may not
487 be present on smaller glaciers because sufficient distance for channels to coalesce is not available. Additionally,
488 mountain glacier environments differ from ice sheet settings due to small scale (e.g., surface debris cover) and
489 large scale (e.g., increased frequency of moraines) topographic heterogeneity. The increased presence of debris
490 on mountain glaciers results in uneven surface albedo, increased surface roughness (Rippin et al., 2015), and
491 additional structural controls on channel formation. For example, large channels often form parallel to medial
492 moraines due to topographic confinement and increased melt in proximity to the debris cover. Drainage network
493 formation is also confined to an often-narrow glacier tongue, whereas channel formation on an ice sheet is often
494 unconfined. On a large scale, meltwater routing in both mountain and ice sheet environments is largely influenced
495 by ice elevation. However, on a smaller scale ice surface structures (e.g., trace crevasses and flow-stripes) exert a
496 strong control meltwater routing, meaning that channels are not always oriented in the same direction (e.g., Figs.
497 5c & 9; Chen et al., in press). The same controls on distribution likely exist in both environments, but the addition
498 of a wider range of variables (e.g., often higher debris cover) in mountain glacier environments makes predicting
499 flow routing more complex.

500 When comparing mountain glacier systems to the SW GrIS (e.g., Smith et al., 2015; Karlstrom & Yang, 2016;
501 Yang & Smith, 2016; Yang et al., 2016, 2021, 2022), there are notable differences in coupling between surface
502 melt and the englacial/subglacial system. On the SW GrIS, virtually all higher-order rivers are observed to
503 terminate in moulins (Smith et al., 2015), whereas in Valais 72 % of main stem channels terminate englacially (37
504 % in crevasses and 35 % in moulins). Additionally, there is a general absence of supraglacial lakes in Valais,
505 except for small lakes on Gorner Glacier and the Aletsch Glacier, whereas they exist in abundance on the GrIS
506 (Chu, 2014). On the GrIS, supraglacial lakes act as temporary storage, with the potential for meltwater to refreeze
507 rather than reaching the terminus each melt season; however, hydro-fracture events can cause rapid lake drainage,
508 which has been linked to ice speed-up events (e.g., Das et al., 2008; Morriss et al., 2013; Chudley et al., 2019). In
509 mountain glacier environments, the general higher surface slopes and absence of temporary supraglacial storage
510 means that proglacial discharge is more clearly linked to rates of surface melt, with very few sudden pulses of
511 increased discharge. The input of surface meltwater to the bed has also been clearly linked to changes in ice flow
512 velocity in mountainous regions (e.g., Willis, 1995; Jobard and Dzikowski, 2006).

513

514 **5.4 Future evolution of supraglacial channel systems**

515 The exact role of climatic warming on supraglacial drainage networks is unknown, but the presence of supraglacial
516 drainage networks at higher elevations can be anticipated in the future due to rising equilibrium lines (Leeson et
517 al., 2015). Whether discharge in current channels will increase or decrease is dependent on the rate of glacier



518 retreat and summer melt. It is likely that larger glaciers will see an increase in channel discharge due to an increase
519 in ablation area (St Germain & Moonman, 2019). However, the reduction in area for smaller glaciers may be large
520 enough to prevent the formation of established drainage networks, and changes in glacier slope may result in a
521 reconfiguration of the drainage system or reduction in drainage density (Fig. 5e). Additionally, glaciers in
522 mountain glacier environments are undergoing an increase in debris cover (e.g., Glasser et al., 2016; Fleischer et
523 al., 2021), and it is not fully understood how changes in debris cover will affect surface meltwater supply and
524 transport, channel morphology and surface albedo (e.g., Leidman et al., 2021). Future research would also benefit
525 from the growing repository of high-resolution orthophoto surveys to inform our understanding of supraglacial
526 hydrology outside of ice sheet settings, particularly concerning seasonal and interannual channel evolution to
527 better inform modelling of glacier hydrology. It is not currently known how widely applicable our research is to
528 regions with larger glaciers and lower rates of surface lowering (e.g., the Arctic) so future studies may benefit
529 from assessing their similarity.

530

531 **6 Conclusion**

532 This study presents the first comprehensive dataset of the distribution and characteristics of supraglacial channels
533 at a regional scale in a mountain glacier environment. We mapped 1890 channel segments (>0.5 m wide) on 85
534 glaciers found to contain channels above our mapping resolution (~0.5 m wide) in Valais Canton, Switzerland,
535 out of a total sample of 285 glaciers. We found large variability in channel drainage densities across glaciers, with
536 the highest drainage densities existing on glaciers characterised by lower relief slopes, with a large portion of their
537 mass at lower elevations (Fig. 7). We find that the presence of channels is primarily dictated by a sufficiently large
538 supply of meltwater (i.e., large enough glacier area) and uninterrupted distance for meltwater to coalesce (i.e.,
539 absence of crevasses and low ice surface slopes). The primary control on channel distribution is surface
540 topography, with the slope and size of the ablation area providing a clear limit on where channels can form and
541 their length (Fig. 5b). However, strong structural controls on channel distribution exist (e.g., crevasse routing and
542 medial moraines).

543 The majority of glaciers are characterised by channels that reach the glacier margin, with the percentage of
544 channels terminating in each position averaged by glacier revealing that on average 80 % of channels run directly
545 off the glacier, and 20 % terminate englacially. Overall, 48 % of glaciers contain no englacially terminating
546 channels, compared to only 3.5 % of glaciers where all channels terminate englacially. The variation in where
547 channels are located and the variation in their terminus environment (moulin/crevasse versus running off the
548 glacier) may result in a range of lag times in proglacial discharge in response to surface melt, with different glacier
549 geometries likely predictive of glacier drainage density and channel pathways (Fig. 7). This differs from typical
550 ice sheet settings where very few supraglacial channels reach the ice margin, with most surface melt transported
551 englacially through crevasses or moulins. In comparison to ice sheets, channel drainage networks in mountain
552 glacier environments are often less established due to glaciers having smaller drainage areas and there being less
553 distance for channels to coalesce, with valley glaciers often narrowing down-glacier reducing the possible size of
554 drainage networks. Channels in Valais are typically characterised by low sinuosity (Fig. 5a), with a general
555 absence of the canyon-like channels described on cold or polythermal glaciers. However, some highly sinuous



556 channels exist, particularly on debris-covered glaciers characterised by channels with steep ice cliffs and on low
 557 slope termini, with sinuous channels most commonly occurring where channels are also deeply incised. Lastly,
 558 further in-situ measurements would be beneficial to determine whether the channels delineated as part of this
 559 study represent the majority of meltwater transport on mountain glaciers, or whether channels below our mapping
 560 resolution also play a key role in meltwater transport.

561

562 **7 Appendix**

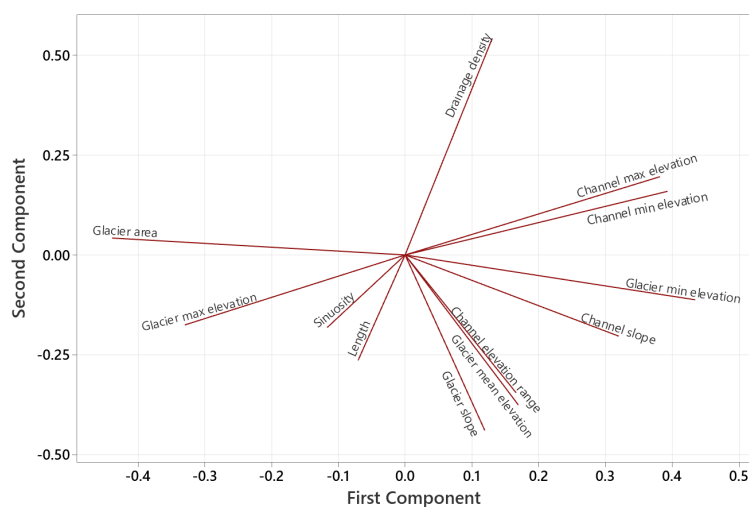
563 **Appendix 1: Principal Component Analysis**

564 **Table A1: The eigenvectors for principal components 1 to 6 from a PCA analysis of glacier and channel**
 565 **characteristics, with PC1 being the most significant. The three largest loadings for each principal**
 566 **component are in bold.**

567

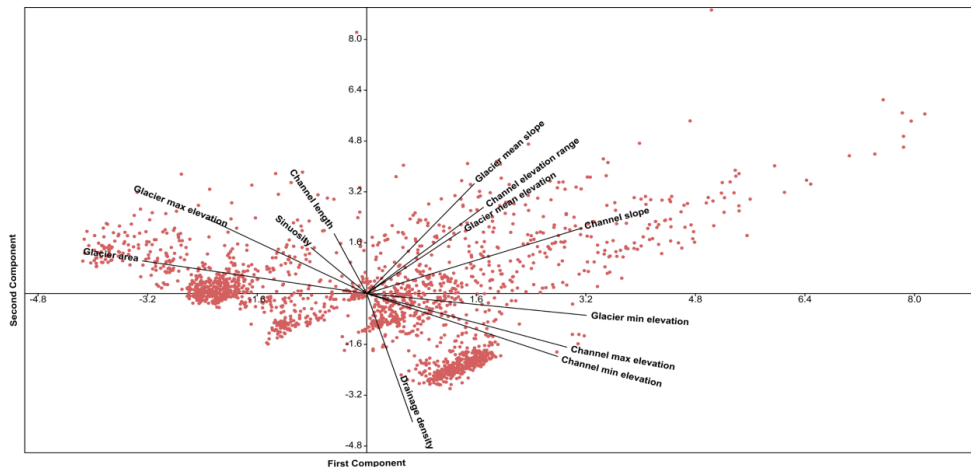
	PC1	PC2	PC3	PC4	PC5	PC6
Glacier area	-0.439	0.042	0.034	0.288	-0.187	0.054
Glacier minimum elevation	0.435	-0.112	0.085	-0.098	0.407	-0.178
Channel maximum elevation	0.393	0.159	0.066	0.436	-0.115	0.186
Channel length	-0.070	-0.264	-0.582	0.312	0.195	-0.199
Channel minimum elevation	0.382	0.196	0.121	0.423	-0.100	0.196
Channel sinuosity	-0.117	-0.182	-0.122	-0.041	0.468	0.845
Channel elevation range	0.166	-0.345	-0.542	0.198	-0.173	-0.068
Channel slope	0.320	-0.203	-0.066	-0.115	-0.483	0.255
Drainage density	0.131	0.543	-0.268	-0.009	0.041	0.083
Mean glacier slope	0.119	-0.439	0.136	-0.309	-0.335	0.141
Glacier mean elevation	0.170	-0.376	0.401	0.280	0.339	-0.188
Glacier max elevation	-0.330	-0.175	0.264	0.462	-0.163	0.086

568
 569
 570
 571
 572
 573



574
575
576
577
578

Figure A1: loading plot for principal components 1 and 2 from a PCA analysis of glacier and channel characteristics.



579
580
581
582
583
584

Figure A2: A biplot from a PCA analysis showing principal components 1 and 2, which was used for cluster analysis and overlaid with a loading plot (see Fig. A1).

585 Data availability

586 The orthophoto and DEM data used in this study are freely available on the SwissTopo website
587 (<https://www.swisstopo.admin.ch/>). Outlines of glaciers in Valais were obtained from Glacier Monitoring in
588 Switzerland (GLAMOS) and are available online (<https://glamos.ch/>). The produced supraglacial channel data is
589 available upon request from the corresponding author (Holly Wytiahłowsky:
590 holly.e.wytiahłowsky@durham.ac.uk).



591 **Author contributions**

592 All authors contributed to the conceptualisation of this project. HW conducted the mapping, formal analysis and
593 data visualisation under the supervision of CRS, RAH, CCC and SSRJ. HW led manuscript writing with comments
594 and revisions provided by all authors.

595

596 **Competing interests**

597 One author is a member of the editorial board of The Cryosphere.

598

599 **Acknowledgements**

600 This work was supported by the Natural Environment Research Council via an IAPETUS2 PhD studentship held
601 by Holly Wytiahlowky (grant reference NE/S007431/1). We thank SwissTopo for making their orthophotos and
602 DEM data open access.

603

604 **8 References**

- 605 Bamber, J. L., Oppenheimer, M., Kopp, R. E., Aspinall, W. P., and Cooke, R. M.: Ice sheet contributions to
606 future sea-level rise from structured expert judgment, *Proc. Natl. Acad. Sci.*, 116, 11195–11200,
607 doi:10.1073/pnas.1817205116, 2019.
- 608 Bell, R. E., Chu, W., Kingslake, J., Das, I., Tedesco, M., Tinto, K. J., Zappa, C. J., Frezzotti, M., Boghosian, A.,
609 and Lee, W. S.: Antarctic ice shelf potentially stabilized by export of meltwater in surface river, *Nature*, 544,
610 344–348, doi:10.1038/nature22048, 2017.
- 611 Carey, M., Molden, O. C., Rasmussen, M. B., Jackson, M., Nolin, A. W., and Mark, B. G.: Impacts of glacier
612 recession and declining meltwater on mountain societies, *Ann. Am. Assoc. Geogr.*, 107, 350–359,
613 doi:10.1080/24694452.2016.1243039, 2017.
- 614 Chen, J., Hodge, R.A., Jamieson, S.S.R. and Stokes, C.R.: Distribution and morphometry of supraglacial
615 channel networks on Antarctic ice shelves. *J. Glaciol.* (in press)
- 616 Chu, V. W.: Greenland Ice Sheet hydrology: A review, *Prog. Phys. Geogr.*, 38, 19–54,
617 doi:10.1177/0309133313507075, 2014.
- 618 Chudley, T. R., Christoffersen, P., Doyle, S. H., Bougamont, M., Schoonman, C. M., Hubbard, B., and James,
619 M. R.: Supraglacial lake drainage at a fast-flowing Greenlandic outlet glacier, *Proc. Natl. Acad. Sci.*, 116,
620 25468–25477, doi:10.1073/pnas.1913685116, 2019.
- 621 Clason, C., Rangecroft, S., Owens, P. N., Łokas, E., Baccolo, G., Selmes, N., Beard, D., Kitch, J., Dextre, R. M.,
622 Morera, S., and Blake, W.: Contribution of glaciers to water, energy and food security in mountain regions:
623 current perspectives and future priorities, *Ann. Glaciol.*, 63, 73–78, doi:10.1017/aog.2023.14, 2023.
- 624 Das, S. B., Joughin, I., Behn, M. D., Howat, I. M., King, M. A., Lizarralde, D., and Bhatia, M. P.: Fracture
625 propagation to the base of the Greenland Ice Sheet during supraglacial lake drainage, *Science*, 320, 778–781,
626 doi:10.1126/science.1153360, 2008.
- 627 Davaze, L., Rabatel, A., Dufour, A., Hugonnet, R., and Arnaud, Y.: Region-wide annual glacier surface mass
628 balance for the European Alps from 2000 to 2016, *Front. Earth Sci.*, 8, doi:10.3389/feart.2020.00149, 2020.



- 629 Delaney, I. and Adhikari, S.: Increased subglacial sediment discharge in a warming climate: consideration of ice
630 dynamics, glacial erosion, and fluvial sediment transport, *Geophys. Res. Lett.*, 47, e2019GL085672,
631 doi:10.1029/2019GL085672, 2020.
- 632 Dozier, J.: An examination of the variance minimization tendencies of a supraglacial stream, *J. Hydrol.*, 31,
633 359–380, doi:10.1016/0022-1694(76)90134-7, 1976.
- 634 Edwards, T. L., Nowicki, S., Marzeion, B., Hock, R., Goelzer, H., Seroussi, H., Jourdain, N. C., Slater, D. A.,
635 Turner, F. E., Smith, C. J., McKenna, C. M., Simon, E., Abe-Ouchi, A., Gregory, J. M., Larour, E., Lipscomb, W.
636 H., Payne, A. J., Shepherd, A., Agosta, C., Alexander, P., Albrecht, T., Anderson, B., Asay-Davis, X.,
637 Aschwanden, A., Barthel, A., Bliss, A., Calov, R., Chambers, C., Champollion, N., Choi, Y., Cullather, R.,
638 Cuzzone, J., Dumas, C., Felikson, D., Fettweis, X., Fujita, K., Galton-Fenzi, B. K., Gladstone, R., Gолledge, N.
639 R., Greve, R., Hattermann, T., Hoffman, M. J., Humbert, A., Huss, M., Huybrechts, P., Immerzeel, W., Kleiner,
640 T., Kraaijenbrink, P., Le clec'h, S., Lee, V., Leguy, G. R., Little, C. M., Lowry, D. P., Malles, J.-H., Martin, D. F.,
641 Maussion, F., Morlighem, M., O'Neill, J. F., Nias, I., Pattyn, F., Pelle, T., Price, S. F., Quiquet, A., Radić, V.,
642 Reese, R., Rounce, D. R., Rückamp, M., Sakai, A., Shafer, C., Schlegel, N.-J., Shannon, S., Smith, R. S.,
643 Straneo, F., Sun, S., Tarasov, L., Trusel, L. D., Van Breedam, J., van de Wal, R., van den Broeke, M.,
644 Winkelmann, R., Zekollari, H., Zhao, C., Zhang, T., and Zwinger, T.: Projected land ice contributions to twenty-
645 first-century sea level rise, *Nature*, 593, 74–82, doi:10.1038/s41586-021-03302-y, 2021.
- 646 Esri. “Imagery” [basemap]. Scale Not Given. “World Imagery”. October 10, 2024.
647 <https://www.arcgis.com/home/item.html?id=10df2279f9684e4a9f6a7f08febac2a9>. (October 22, 2024)
- 648 Ferguson, R. I.: Sinuosity of supraglacial streams, *Geol. Soc. Am. Bull.*, 84, 251–256, doi:10.1130/0016-
649 7606(1973)84<251:SOSS>2.0.CO;2, 1973.
- 650 Fischer, M., Huss, M., and Hoelzle, M.: Surface elevation and mass changes of all Swiss glaciers 1980–2010,
651 *Cryosphere*, 9, 525–540, doi:10.5194/tc-9-525-2015, 2015.
- 652 Fleischer, F., Otto, J.-C., Junker, R. R., and Hölbling, D.: Evolution of debris cover on glaciers of the Eastern
653 Alps, Austria, between 1996 and 2015, *Earth Surf. Process. Landf.*, 46, 1673–1691, doi:10.1002/esp.5065, 2021.
- 654 Fyffe, C. L., Brock, B. W., Kirkbride, M. P., Mair, D. W. F., Arnold, N. S., Smiraglia, C., Diolaiuti, G., and
655 Diotri, F.: Do debris-covered glaciers demonstrate distinctive hydrological behaviour compared to clean
656 glaciers?, *J. Hydrol.*, 570, 584–597, doi:10.1016/j.jhydrol.2018.12.069, 2019.
- 657 Glasser, N. F., Holt, T. O., Evans, Z. D., Davies, B. J., Pelto, M., and Harrison, S.: Recent spatial and temporal
658 variations in debris cover on Patagonian glaciers, *Geomorphology*, 273, 202–216,
659 doi:10.1016/j.geomorph.2016.07.036, 2016.
- 660 Gleason, C. J., Smith, L. C., Chu, V. W., Legleiter, C. J., Pitcher, L. H., Overstreet, B. T., Rennermalm, A. K.,
661 Forster, R. R., and Yang, K.: Characterizing supraglacial meltwater channel hydraulics on the Greenland Ice
662 Sheet from in situ observations, *Earth Surf. Process. Landf.*, 41, 2111–2122, doi:10.1002/esp.3977, 2016.
- 663 Gleason, C. J., Yang, K., Feng, D., Smith, L. C., Liu, K., Pitcher, L. H., Chu, V. W., Cooper, M. G., Overstreet,
664 B. T., Rennermalm, A. K., and Ryan, J. C.: Hourly surface meltwater routing for a Greenlandic supraglacial
665 catchment across hillslopes and through a dense topological channel network, *Cryosphere*, 15, 2315–2331,
666 doi:10.5194/tc-15-2315-2021, 2021.
- 667 Gulley, J. D., Benn, D. I., Mueller, D., and Luckman, A.: A cut-and-closure origin for englacial conduits in
668 uncrevassed regions of polythermal glaciers, *J. Glaciol.*, 55, 66–80, doi:10.3189/002214309788608930, 2009.
- 669 Hambrey, M. J.: Supraglacial drainage and its relationship to structure, with particular reference to Charles
670 Rabots Bre, Okstindan, Norway, *Nor. Geogr. Tidsskr.*, 31, 69–77, doi:10.1080/00291957708545319, 1977.
- 671 Hock, R., Iken, L., and Wangler, A.: Tracer experiments and borehole observations in the over-deepening of
672 Aletschgletscher, Switzerland, *Ann. Glaciol.*, 28, 253–260, doi:10.3189/172756499781821742, 1999.
- 673 Horton, R. E.: Erosional development of streams and their drainage basins; hydrophysical approach to
674 quantitative morphology, *Geol. Soc. Am. Bull.*, 56, 275–370, doi:10.1130/0016-
675 7606(1945)56[275:EDOSAT]2.0.CO;2, 1945.



- 676 Hugonnet, R., McNabb, R., Berthier, E., Menounos, B., Nuth, C., Girod, L., Farinotti, D., Huss, M., Dussaillant,
677 I., Brun, F., and Kääh, A.: Accelerated global glacier mass loss in the early twenty-first century, *Nature*, 592,
678 726–731, doi:10.1038/s41586-021-03436-z, 2021.
- 679 Immerzeel, W. W., Lutz, A. F., Andrade, M., Bahl, A., Biemans, H., Bolch, T., Hyde, S., Brumby, S., Davies, B.
680 J., Elmore, A. C., Emmer, A., Feng, M., Fernández, A., Haritashya, U., Kargel, J. S., Koppes, M., Kraaijenbrink,
681 P. D. A., Kulkarni, A. V., Mayewski, P. A., Nepal, S., Pacheco, P., Painter, T. H., Pellicciotti, F., Rajaram, H.,
682 Rupper, S., Sinisalo, A., Shrestha, A. B., Viviroli, D., Wada, Y., Xiao, C., Yao, T., and Baillie, J. E. M.:
683 Importance and vulnerability of the world’s water towers, *Nature*, 577, 364–369, doi:10.1038/s41586-019-1822-
684 y, 2020.
- 685 Irvine-Fynn, T. D. L., Hodson, A. J., Moorman, B. J., Vatne, G., and Hubbard, A. L.: Polythermal glacier
686 hydrology: a review, *Rev. Geophys.*, 49, doi:10.1029/2010RG000350, 2011.
- 687 Isenko, E., Naruse, R., and Mavlyudov, B.: Water temperature in englacial and supraglacial channels: Change
688 along the flow and contribution to ice melting on the channel wall, *Cold Reg. Sci. Technol.*, 42, 53–62,
689 doi:10.1016/j.coldregions.2004.12.003, 2005.
- 690 Jobard, S. and Dzikowski, M.: Evolution of glacial flow and drainage during the ablation season, *J. Hydrol.*,
691 330, 663–671, doi:10.1016/j.jhydrol.2006.04.031, 2006.
- 692 Karlstrom, L. and Yang, K.: Fluvial supraglacial landscape evolution on the Greenland Ice Sheet, *Geophys. Res.*
693 *Let.*, 43, 2683–2692, doi:10.1002/2016GL067697, 2016.
- 694 Khan, A. L., Xian, P., and Schwarz, J. P.: Black carbon concentrations and modeled smoke deposition fluxes to
695 the bare-ice dark zone of the Greenland Ice Sheet, *Cryosphere*, 17, 2909–2918, doi:10.5194/tc-17-2909-2023,
696 2023.
- 697 King, L., Hassan, M. A., Yang, K., and Flowers, G.: Flow routing for delineating supraglacial meltwater channel
698 networks, *Remote Sens.*, 8, 988, doi:10.3390/rs8120988, 2016.
- 699 Kingslake, J., Ely, J. C., Das, I., and Bell, R. E.: Widespread movement of meltwater onto and across Antarctic
700 ice shelves, *Nature*, 544, 349–352, doi:10.1038/nature22049, 2017.
- 701 Kneib, M., Fyffe, C. L., Miles, E. S., Lindemann, S., Shaw, T. E., Buri, P., McCarthy, M., Ouvry, B., Vieli, A.,
702 Sato, Y., Kraaijenbrink, P. D. A., Zhao, C., Molnar, P., and Pellicciotti, F.: Controls on ice cliff distribution and
703 characteristics on debris-covered glaciers, *Geophys. Res. Lett.*, 50, e2022GL102444,
704 doi:10.1029/2022GL102444, 2023.
- 705 Knighton, A. D.: Channel form adjustment in supraglacial streams, Austre Okstindbreen, Norway, *Arct. Antarct.*
706 *Alp. Res.*, 17, 451, doi:10.2307/1550870, 1985.
- 707 Knighton, A. D.: Channel form and flow characteristics of supraglacial streams, Austre Okstindbreen, Norway,
708 *Arct. Alp. Res.*, 13, 295, doi:10.2307/1551036, 1981.
- 709 Knighton, A. D.: Meandering habit of supraglacial streams, *Geol. Soc. Am. Bull.*, 83, 201–204,
710 doi:10.1130/0016-7606(1972)83[201:MHOSS]2.0.CO;2, 1972.
- 711 Leeson, A. A., Shepherd, A., Briggs, K., Howat, I., Fettweis, X., Morlighem, M., and Rignot, E.: Supraglacial
712 lakes on the Greenland Ice Sheet advance inland under warming climate, *Nat. Clim. Change*, 5, 51–55,
713 doi:10.1038/nclimate2463, 2015.
- 714 Leidman, S. Z., Rennermalm, Å. K., Muthyala, R., Guo, Q., and Overeem, I.: The presence and widespread
715 distribution of dark sediment in Greenland Ice Sheet supraglacial streams implies substantial impact of
716 microbial communities on sediment deposition and albedo, *Geophys. Res. Lett.*, 48, 2020GL088444,
717 doi:10.1029/2020GL088444, 2021.
- 718 Leigh, J. R., Stokes, C. R., Carr, R. J., Evans, I. S., Andreassen, L. M., and Evans, D. J. A.: Identifying and
719 mapping very small (<0.5 km²) mountain glaciers on coarse to high-resolution imagery, *J. Glaciol.*, 65, 873–
720 888, <https://doi.org/10.1017/jog.2019.50>, 2019.



- 721 Leinss, S. and Bernhard, P.: TanDEM-X: Deriving InSAR height changes and velocity dynamics of Great
722 Aletsch Glacier, *IEEE J. Sel. Top. Appl. Earth Obs. Remote Sens.*, 14, 4798–4815,
723 <https://doi.org/10.1109/JSTARS.2021.3078084>, 2021.
- 724 Linsbauer, A., Huss, M., Hodel, E., Bauder, A., Fischer, M., Weidmann, Y., Bärtschi, H., and Schmassmann, E.:
725 The new Swiss glacier inventory SGI2016: from a topographical to a glaciological dataset, *Front. Earth Sci.*, 9,
726 [doi:10.3389/feart.2021.704189](https://doi.org/10.3389/feart.2021.704189), 2021.
- 727 Mantelli, E., Camporeale, C., and Ridolfi, L.: Supraglacial channel inception: modeling and processes, *Water
728 Resour. Res.*, 51, 7044–7063, [doi:10.1002/2015WR017075](https://doi.org/10.1002/2015WR017075), 2015.
- 729 Marston, R. A.: Supraglacial stream dynamics on the Juneau Icefield, *Ann. Am. Assoc. Geogr.*, 73, 597–608,
730 [doi:10.1111/j.1467-8306.1983.tb01861.x](https://doi.org/10.1111/j.1467-8306.1983.tb01861.x), 1983.
- 731 MeteoSwiss: <https://www.meteoswiss.admin.ch/>, last access: 1 February 2024.
- 732 Mölg, N., Bolch, T., Walter, A., and Vieli, A.: Unravelling the evolution of Zmuttgletscher and its debris cover
733 since the end of the Little Ice Age, *Cryosphere*, 13, 1889–1909, [doi:10.5194/tc-13-1889-2019](https://doi.org/10.5194/tc-13-1889-2019), 2019.
- 734 Moore, R. C.: Origin of Inclosed Meanders on Streams of the Colorado Plateau, *J. Glaciol.*, 34, 29–57,
735 [doi:10.1086/623270](https://doi.org/10.1086/623270), 1926.
- 736 Morriss, B. F., Hawley, R. L., Chipman, J. W., Andrews, L. C., Catania, G. A., Hoffman, M. J., Lüthi, M. P., and
737 Neumann, T. A.: A ten-year record of supraglacial lake evolution and rapid drainage in West Greenland using an
738 automated processing algorithm for multispectral imagery, *Cryosphere*, 7, 1869–1877, [doi:10.5194/tc-7-1869-
739 2013](https://doi.org/10.5194/tc-7-1869-2013), 2013.
- 740 Nienow, P., Sharp, M., and Willis, I.: Seasonal changes in the morphology of the subglacial drainage system,
741 Haut Glacier d’Arolla, Switzerland, *Earth Surf. Process. Landf.*, 23, 825–843,
742 [https://doi.org/10.1002/\(SICI\)1096-9837\(199809\)23:9<825::AID-ESP893>3.0.CO;2-2](https://doi.org/10.1002/(SICI)1096-9837(199809)23:9<825::AID-ESP893>3.0.CO;2-2), 1998.
- 743 Pitcher, L. H. and Smith, L. C.: Supraglacial Streams and Rivers, *Annu. Rev. Earth Planet. Sci.*, 47, 421–452,
744 [doi:10.1146/annurev-earth-053018-060212](https://doi.org/10.1146/annurev-earth-053018-060212), 2019.
- 745 Rippin, D. M., Pomfret, A., and King, N.: High resolution mapping of supra-glacial drainage pathways reveals
746 link between micro-channel drainage density, surface roughness and surface reflectance, *Earth Surf. Process.
747 Landf.*, 40, 1279–1290, [doi:10.1002/esp.3719](https://doi.org/10.1002/esp.3719), 2015.
- 748 Rounce, D. R., Hock, R., Maussion, F., Hugonnet, R., Kochitzky, W., Huss, M., Berthier, E., Brinkerhoff, D.,
749 Compagno, L., Copland, L., Farinotti, D., Menounos, B., and McNabb, R. W.: Global glacier change in the 21st
750 century: Every increase in temperature matters, *Science*, 379, 78–83, [doi:10.1126/science.abo1324](https://doi.org/10.1126/science.abo1324), 2023.
- 751 Ryan, J. C., Hubbard, A., Stibal, M., Irvine-Fynn, T. D., Cook, J., Smith, L. C., Cameron, K., and Box, J.: Dark
752 zone of the Greenland Ice Sheet controlled by distributed biologically-active impurities, *Nat. Commun.*, 9, 1065,
753 [doi:10.1038/s41467-018-03353-2](https://doi.org/10.1038/s41467-018-03353-2), 2018.
- 754 Seaberg, S. Z., Seaberg, J. Z., Hooke, R. L., and Wiberg, D. W.: Character of the englacial and subglacial
755 drainage system in the lower part of the ablation area of Storglaciären, Sweden, as Revealed by Dye-Trace
756 Studies, *J. Glaciol.*, 34, 217–227, [doi:10.3189/S0022143000032263](https://doi.org/10.3189/S0022143000032263), 1988.
- 757 Shepherd, R. G.: Incised river meanders: evolution in simulated bedrock, *Science*, 178, 409–411,
758 [doi:10.1126/science.178.4059.409](https://doi.org/10.1126/science.178.4059.409), 1972.
- 759 Smith, L. C., Chu, V. W., Yang, K., Gleason, C. J., Pitcher, L. H., Rennermalm, A. K., Legleiter, C. J., Behar, A.
760 E., Overstreet, B. T., Moustafa, S. E., Tedesco, M., Forster, R. R., LeWinter, A. L., Finnegan, D. C., Sheng, Y.,
761 and Balog, J.: Efficient meltwater drainage through supraglacial streams and rivers on the southwest Greenland
762 Ice Sheet, *Proc. Natl. Acad. Sci.*, 112, 1001–1006, [doi:10.1073/pnas.1413024112](https://doi.org/10.1073/pnas.1413024112), 2015.
- 763 Sommer, C., Malz, P., Seehaus, T. C., Lippl, S., Zemp, M., and Braun, M. H.: Rapid glacier retreat and
764 downwasting throughout the European Alps in the early 21st century, *Nat. Commun.*, 11, 3209,
765 [doi:10.1038/s41467-020-16818-0](https://doi.org/10.1038/s41467-020-16818-0), 2020.



- 766 St Germain, S. L. and Moorman, B. J.: Long-term observations of supraglacial streams on an Arctic glacier, *J.*
767 *Glaciol.*, 65, 900–911, doi:10.1017/jog.2019.60, 2019.
- 768 Swift, D. A., Nienow, P. W., Spedding, N., and Hoey, T. B.: Geomorphic implications of subglacial drainage
769 configuration: rates of basal sediment evacuation controlled by seasonal drainage system evolution, *Sediment.*
770 *Geol.*, 149, 5–19, doi:10.1016/S0037-0738(01)00241-X, 2002.
- 771 Tepes, P., Gourmelen, N., Nienow, P., Tsamados, M., Shepherd, A., and Weissgerber, F.: Changes in elevation
772 and mass of Arctic glaciers and ice caps, 2010–2017, *Remote Sens. Environ.*, 261, 112481,
773 doi:10.1016/j.rse.2021.112481, 2021.
- 774 Turowski, J. M.: Alluvial cover controlling the width, slope and sinuosity of bedrock channels, *Earth Surf. Dyn.*,
775 6, 29–48, doi:10.5194/esurf-6-29-2018, 2018.
- 776 Willis, I.C.: Intra-annual variations in glacier motion: a review, *Prog. Phys. Geogr.*, 19,
777 doi:10.1177/030913339501900104, 1995.
- 778 Wouters, B., Gardner, A. S., and Moholdt, G.: Global glacier mass loss during the GRACE satellite mission
779 (2002–2016), *Front. Earth Sci.*, 7, 2019.
- 780 Yang, K. and Smith, L. C.: Internally drained catchments dominate supraglacial hydrology of the southwest
781 Greenland Ice Sheet, *J. Geophys. Res.-Earth Surf.*, 121, doi:10.1002/2016JF003927, 2016.
- 782 Yang, K. and Smith, L. C.: Supraglacial streams on the Greenland Ice Sheet delineated from combined spectral-
783 shape information in high-resolution satellite imagery, *IEEE Geosci. Remote Sens. Lett.*, 10, 801–805,
784 doi:10.1109/LGRS.2012.2224316, 2013.
- 785 Yang, K., Smith, L. C., Andrews, L. C., Fettweis, X., and Li, M.: Supraglacial drainage efficiency of the
786 Greenland Ice Sheet estimated from remote sensing and climate models, *J. Geophys. Res.-Earth Surf.*, 127,
787 e2021JF006269, doi:10.1029/2021JF006269, 2022.
- 788 Yang, K., Smith, L. C., Chu, V. W., Gleason, C. J., and Li, M.: A caution on the use of surface digital elevation
789 models to simulate supraglacial hydrology of the Greenland Ice Sheet, *IEEE J. Sel. Top. Appl. Earth Observ.*
790 *Remote Sens.*, 8, 5212–5224, doi:10.1109/JSTARS.2015.2483483, 2015.
- 791 Yang, K., Smith, L. C., Chu, V. W., Pitcher, L. H., Gleason, C. J., Rennermalm, A. K., and Li, M.: Fluvial
792 morphometry of supraglacial river networks on the southwest Greenland Ice Sheet, *GISci. Remote Sens.*, 53,
793 459–482, doi:10.1080/15481603.2016.1162345, 2016.
- 794 Yang, K., Smith, L. C., Cooper, M. G., Pitcher, L. H., As, D. van, Lu, Y., Lu, X., and Li, M.: Seasonal evolution
795 of supraglacial lakes and rivers on the southwest Greenland Ice Sheet, *J. Glaciol.*, 67, 592–602,
796 doi:10.1017/jog.2021.10, 2021.
- 797 Yang, K., Smith, L. C., Karlstrom, L., Cooper, M. G., Tedesco, M., van As, D., Cheng, X., Chen, Z., and Li, M.:
798 A new surface meltwater routing model for use on the Greenland Ice Sheet surface, *Cryosphere*, 12, 3791–3811,
799 doi:10.5194/tc-12-3791-2018, 2018.
- 800 Yang, K., Smith, L. C., Sole, A., Livingstone, S. J., Cheng, X., Chen, Z., and Li, M.: Supraglacial rivers on the
801 northwest Greenland Ice Sheet, Devon Ice Cap, and Barnes Ice Cap mapped using Sentinel-2 imagery, *Int. J.*
802 *Appl. Earth Obs. Geoinf.*, 78, 1–13, doi:10.1016/j.jag.2019.01.008, 2019.
- 803 Yang, K., Sommers, A., Andrews, L. C., Smith, L. C., Lu, X., Fettweis, X., and Li, M.: Intercomparison of
804 surface meltwater routing models for the Greenland Ice Sheet and influence on subglacial effective pressures,
805 *Cryosphere*, 14, 3349–3365, doi:10.5194/tc-14-3349-2020, 2020.
- 806 Zekollari, H., Huss, M., and Farinotti, D.: Modelling the future evolution of glaciers in the European Alps under
807 the EURO-CORDEX RCM ensemble, *Cryosphere*, 13, 1125–1146, doi:10.5194/tc-13-1125-2019, 2019.
- 808 Zemp, M., Huss, M., Thibert, E., Eckert, N., McNabb, R., Huber, J., Barandun, M., Machguth, H., Nussbaumer,
809 S. U., Gärtner-Roer, I., Thomson, L., Paul, F., Maussion, F., Kutuzov, S., and Cogley, J. G.: Global glacier mass

<https://doi.org/10.5194/egusphere-2024-3894>

Preprint. Discussion started: 7 January 2025

© Author(s) 2025. CC BY 4.0 License.



810 changes and their contributions to sea-level rise from 1961 to 2016, *Nature*, 568, 382–386, doi:10.1038/s41586-
811 019-1071-0, 2019.

812

813

814